Transport Analysis of Filamentary Dielectric Breakdown Model for Metal-Oxide-Semiconductor Tunnel Structures

David Z.-Y. Ting[†,*] and T. C. McGill*

†Department of Physics, National Tsing Hua University
Hsinchu, Taiwan 30043, Rep. of China
E-mail: dzt@phys.nthu.edu.tw.edu

*Department of Applied Physics,California Institute of Technology
Pasadena, California 91125, U.S.A.
E-mail: dzt@ssdp.caltech.edu; tcm@ssdp.caltech.edu

The current-voltage characteristics of n^+ poly-Si/SiO_2/p-Si tunnel structures containing nano-scale filaments embedded in ultra-thin oxide layers are analyzed using a 3D quantum mechanical scattering calculation. We find that the filaments act as highly efficient localized conduction paths and can lead to dramatic increases in current densities. By using progressively larger filaments, we can reproduce a range of stressed-induced behavior found in experimental current-voltage characteristics, including quasi-breakdown and breakdown. We also find that at below flat-band, the current densities in structure with long filaments are greatly enhanced by resonant tunneling through states identified as quantum dots, and that this current enhancement is highly temperature dependent.

1. Introduction

It is well known that constant current or voltage stressing of metal-oxide-semiconductor (MOS) structures in the Fowler-Nordheim tunneling regime leads to quasi-breakdown or breakdown in ultra-thin oxides characterized by dramatic increases in leakage currents. Based on experimental observations, several groups have proposed the formation of oxide-embedded filaments as a model for breakdown.[1]-[3] In particular, based on experimental studies of interfacial strains, Hirose and co-workers proposed the existence of localized conduction filaments extending for no more than 3 nm from the SiO_2/Si interface into the oxide layer. In this work, we analyze the reverse-bias current-voltage characteristics of MOS tunnel structures containing filaments embedded in ultra-thin oxide layers using 3D quantum mechanical scattering calculations.

2. Model

We analyze the reverse gate bias current-voltage characteristics of n^+ poly-Si/SiO_2/p-Si tunnel structures containing oxide layers embedded with nano-scale filaments. To compute transmission coefficients for these structures, we use the open-boundary planar supercell stack method (OPSSM)[5] which solves quantum mechanical scattering problems exactly for 3D geometries described by planar supercell stacks. We then calculate current densities using the Tsu-Esaki formulation.[6] In our model the ploy-Si conduction band edge is at $E_c^M = 0$, and the Fermi level at $E_F^M = 0.1$ eV. The n^+ poly-Si/SiO_2 interface barrier height is taken as $\Phi^B = 3.25$ eV,[1] and the SiO_2/p-Si conduction band offset 3.29 eV.[7] The p-Si Fermi level is set at 0.88 eV below E_c^{Si}. Thus a gate bias of $V_{FB} = -0.92$ V is required to bring the oxide into flat-band condition. The effective masses of the n^+ poly-Si, SiO_2, and p-Si are taken to be 1.0 m_0, 0.35 m_0, and 0.9 m_0, respectively. For simplicity, we assume flat-band conditions in poly-Si and p-Si.

We consider a set of structures with 4.5 nm thick oxides, embedded with cylindrical filaments 1.55 nm in diameter. Note that the filament we are using in this work are much smaller in cross section than those used in the work of Hirose et al.[1] The filaments account for approximately 2.5% of our computational domain in cross-sectional area, and extend from the SiO_2/Si interface into the oxide layer with cylinder heights of $h = 0.8$, 1.5, and 3.0 nm. A fourth, "undamaged" ($h = 0$) structure is also included for comparison. Because the nature of the filamentary material is not well known, we choose to fill the cylinders with silicon for simplicity. We stress that this scheme is only a convenient way to represent barrier embedded lower potential regions which can be characterize by some transverse and lateral dimensions. This does not nec-

0-7803-4369-7/98 $10.00 ©1998 IEEE

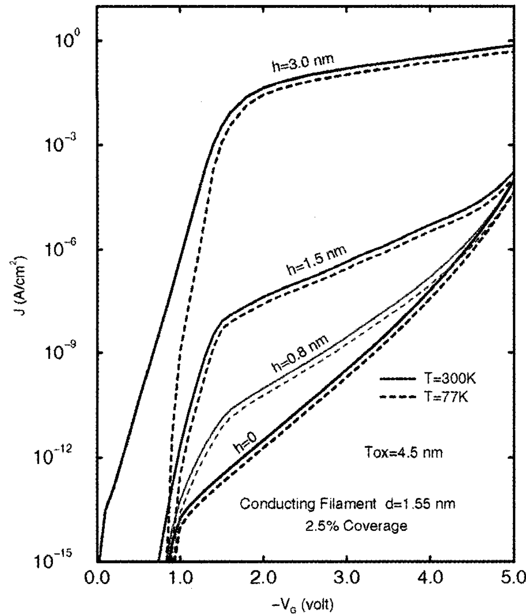

Figure 1: Calculated current density-voltage curves for a set of n^+ poly-Si/SiO_2/p-Si tunnel structures with oxide-embedded cylindrical nano-scale filaments of varying heights (h). At high negative gate bias, the J-V curves for structures with shorter filaments converge, while that for the long-filament structure ($h = 3$ nm) shows much higher current density; these features are reminiscent of pre-breakdown and breakdown behavior observed experimentally. At very low negative gate bias (less than 1V), the $h = 3$ nm structure J-V characteristics also shows strong temperature dependence; this is the result of resonant tunneling through electro-statically confined quantum dot states.

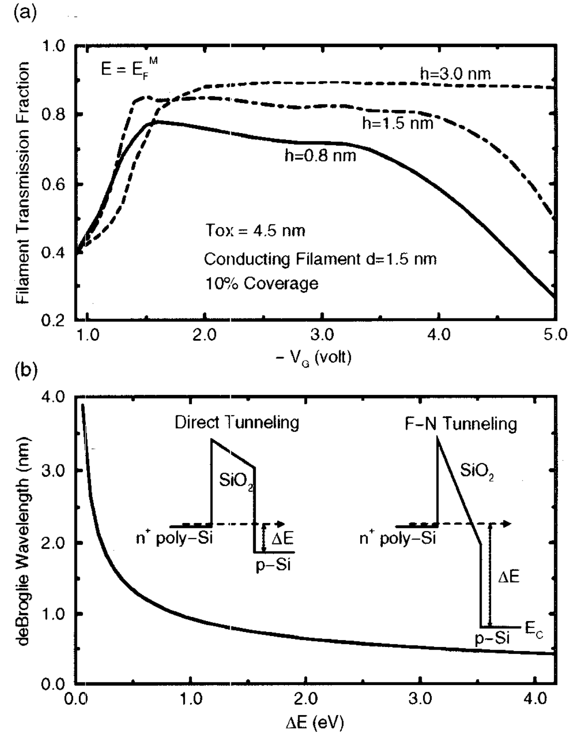

Figure 2: (a) Filament transmission fraction as a function of gate bias calculated from transmitting state wave functions for electrons with incident energy $E = E_F^M$. (b) Electron deBroglie wavelength (λ_e) as a function of excess energy (ΔE) of a coherently tunneling electron upon reaching the p-Si electrode. Insets illustrate band diagrams in the direct and Fowler-Nordheim tunneling regimes.

essarily mean that the oxide layer is literally embedded with silicon filaments, although there has been some experimental evidence identifying breakdown spots in oxides as crystallized silicon.[8]

3. Results

Fig. 1 shows the J-V curves for these structures calculated at 300K and 77K. We note that in general, current densities increase dramatically with filament length h. However, current densities for structures with shorter filaments ($h = 0.8$ and 1.5 nm) converge with that for the undamaged ($h = 0$) structure in the low and high bias limits. This behavior can be understood in terms of lateral localization of transmitting state wave functions in the nano-filaments.

We quantify the degree of lateral localization by defining the filament transmission fraction for a transmitting state as the sum of probability density over the filament sites, divided by the total probability density in the filament containing layers. Fig. 2(a) shows filament transmission fractions as a function of applied bias for tunneling states with incident energy equal to E_F^M (being representative of current-contributing states). The filaments only occupy 2.5% of the cross-sectional area, and in all cases, the fractions greatly exceed that value. The large filament transmission fractions clearly point to localized conduction. The initial rise in the transmission fraction curves can be understood by examining the behavior of tunneling electrons near the SiO_2/p-Si interface where the filaments are anchored. Fig. 2(b) shows that as tunneling electron energy relative to the p-Si side increases with $|V_G|$, a corresponding decrease in the electron deBroglie wavelength λ_e occurs. A smaller λ_e makes it easier for an electron to find its way into the relatively narrow filaments. This translates to stronger lateral confinement, and is responsible for the initial rise found in Fig. 2(a). Direct examination of tunneling state wave functions (Fig. 3) reveals that the filaments act as highly efficient localized conduction paths. Confinement remains strong until the device is biased into the Fowler-Nordheim regime ($|V_G| > 4$V), where it weakens significantly for the shorter filaments. This is because in the Fowler-Nordheim regime the trailing edge of the oxide does not act as a confining barrier since its band edge is biased below the energy of the tunneling electron, as illustrated in the inset of Fig. 2(b).

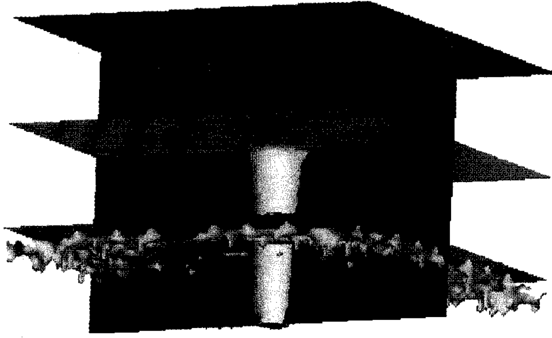

Figure 3: The wave function of a tunneling state represented as a white isosurfaces of constant probability densities. A cross-section of the metal(light blue)-oxide(red)-semiconductor(blue) structure containing the nano-filament is shown simultaneously for reference. Note the localization of the tunneling state wave function in the nano-filament in the center of the picture.

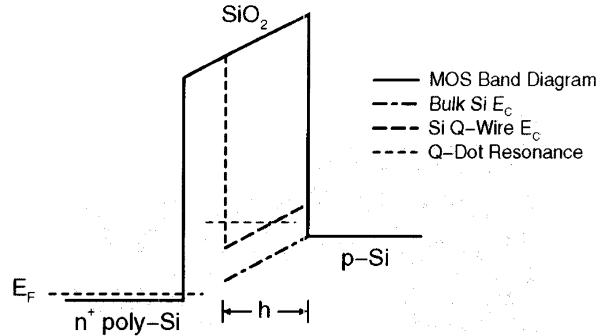

Figure 4: Schematic band diagram for an n^+ poly-Si/SiO_2/p-Si tunnel structure with embedded nano-filaments at low bias ($|V_G| < |V_{FB}|$).

We can now explain Fig. 1. At biases just above flat-band voltage ($\sim$ 1V), λ_e of a typical tunneling electron is larger than the filament diameter. Thus electrons are only weakly localized, and cannot take full advantage of filamentary conduction paths. Therefore current densities do not depend strongly on filament length (we will discuss the exceptional case of h = 3nm below.). Further into the direct tunneling regime, λ_e decreases, and electrons now can be highly localized in the filaments. Since the oxide barrier in front of a longer filament is thinner, current densities show exponential increase with filament length. In the Fowler-Nordheim regime the tunneling properties are primarily determined by the leading edge of the oxide barrier. Thus the $h = 0.8$ and 1.5 nm structures, with their (short) filaments located near the trailing interface, show current densities which converge with that of the undamaged ($h = 0$) structure at high bias. The filaments in the $h = 3.0$ nm structure extend sufficiently close to the leading edge of the tunnel barrier so that the excess current density persists even at higher biases.

The exception to our explanations above is the behavior of the 300K J-V curve for the $h = 3.0$ nm structure at lower biases ($|V_G| < |V_{FB}|$), where the current densities are anomalously high due to resonant tunneling through quantum dot states. Fig. 4 shows a low bias band diagram. Since $|V_G| < |V_{FB}|$, the band edge is actually higher on the p-Si side. Because the oxide contains Si filaments, we have also drawn in the band edge of Si. Note however that the band edge seen by an electron in the Si filament is not the bulk Si band edge since the filament really should be thought of as a truncated quantum wire. Therefore the additional energy due to lateral quantization must be taken into consideration. We have schematically indicated this in the figure as the "Si Q-Wire Ec." This then gives us in the third (perpendicular) direction a double barrier potential, which, along with the filament walls, form a 3D quantum dot potential. The wave function of such a quantum dot is shown in Fig. 5. Resonant tunneling through quantum dot states greatly enhance transmission probability in this regime. However, this effect is highly temperature dependent since resonances must be above the p-Si band edge to carry current, and only electrons with energy many k_BT's above the chemical potential in the incoming electrode can take advantage of them. This accounts for the low bias temperature dependence of the $h = 3.0$ nm structure.

To study the dependence on the fractional gate area occupation, we kept the same filament geometry as before, but decrease filament density by a factor of four. We find that except for short filaments under high biases (Fowler-Nordheim tunneling currents are determined by the leading edge of the tunnel barrier; short filaments only play a minor role.), current density scales remarkably well with filament density, indicating that the filaments are highly efficient localized conduction paths. We have also examined a case where we fixed the fractional gate area occupied by filaments, but varied the filament diameter. Fig. 6 shows that for a given filament height, the current densities become approximately independent of d for $|V_G|$ exceeding 2.5 to 3.5 volts (higher for longer filaments). This is because as λ_e in the filament becomes significantly smaller than d under sufficiently high biases, transmission amplitude becomes proportional to filament cross-sectional area coverage. Below these biases, however, current densities typically show sizable increase with d. In the case of $d = 3.10$ nm, the J-V curves for various filament length h no longer converge at low biases.

4. Summary

We analyze the reverse-bias current-voltage characteristics of MOS tunnel structures containing nano-scale filaments embedded in ultra-thin oxide layers using 3D quantum mechanical scattering calculations. We model the nano-filaments using cylinders which can be conveniently characterized by their heights (h) and diameters (d). Scaling studies and direct examination of tunneling state wave functions (Fig. 3) show that the filaments act as highly efficient localized conduction

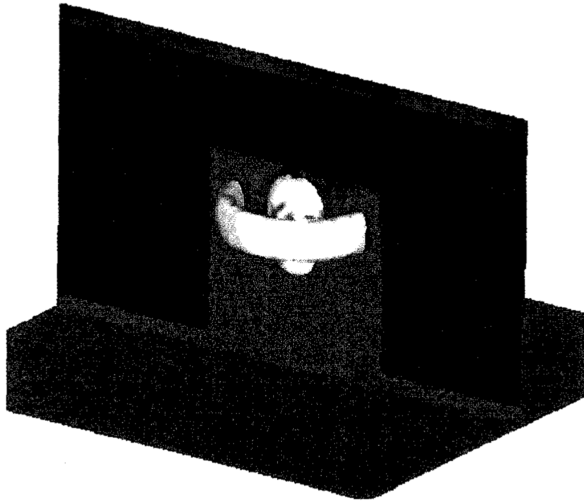

Figure 5: A transmitting resonant tunneling state wave function showing a quantum dot trapped at the tip of a cylindrically filament. The trapping is in part due to the electrostatic potential found for reversed gate bias lower than flat-band voltage.

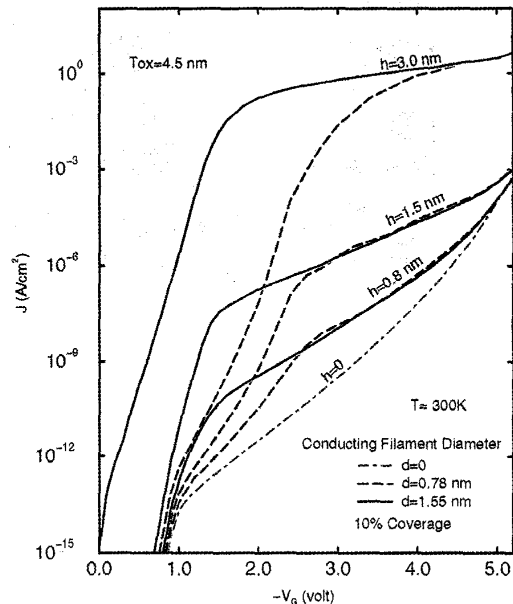

Figure 6: Calculated current density-voltage curves for a set of n^+ poly-Si/SiO_2/p-Si tunnel structures with oxide-embedded cylindrical nano-filaments of various diameters (d) and heights (h). Note that the larger diameter (d = 1.55 nm) data set shows separation of J-V curves at low reverse gate bias, while the small diameter data set does not.

paths which can lead to dramatic increases in current densities. By using different filament sizes, we can produce simulated current-voltage characteristics which bear strong qualitatively resemblance to those observed experimentally for quasi-breakdown and breakdown[3, 4] cases. We find that stress-induced behavior at low biases and high biases, respectively, are best simulated using cylinders with progressively larger diameters and heights. (Figs. 1,6) By comparing our simulations to experimental results, we conclude that for quasi-breakdown, the filaments must be sufficiently short so that they do not penetrate the leading edge of the oxide layer. And for the breakdown case, filaments must be long and wide so that substantial current density increases may be obtained at both low and high biases. We also find that under very low reverse gate bias (below flat-band), current densities in structure with long filaments are greatly enhanced by resonant tunneling through states identified as electro-statically localized quantum dots (Fig. 5), and that this current enhancement is highly temperature dependent (Fig. 1).

Acknowledgement

The author thanks O. J. Marsh, and, E. S. Daniel for helpful discussions, and M. A. Barton for technical assistance. This work was supported by the ROC National Science Council under Grant No. NSC 87-2112-M-007-005, the U. S. Office of Naval Research (ONR) under Grant No. N00014-89-J-1141, and the Defense Advanced Research Projects Agency (DARPA) monitored by U. S. Air Force Office of Scientific Research (AFOSR) under Grant No. F49620-96-1-0021.

References

[1] M. Hirose, J. L. Alay, T. Yoshida and S. Miyazaki, in *The Physics and Chemistry of SiO_2 and the Si-SiO_2 interface - 3*, H. Z. Massoud, E. H. Poindexter, and C. R. Helms, Ed., The Electrochemical Society, NJ, 1996, Proc. Vol. 96-1, pp. 485-496.

[2] Pushkar P. Apte and Krishna C. Saraswat, *IEEE Transactions on Electron Devices* Vol. 41, 1595(1994).

[3] A. Halimaoui, O. Brière, and G. Ghibaudo, *Microelectronic Engineering* Vol. 36, 157(1997).

[4] M. Depas, T. Nigam, and M. M. Heyns, *IEEE Transactions on Electron Devices* Vol. 43, 1499(1996).

[5] D. Z.-Y. Ting, S. K. Kirby, and T. C. McGill, *J. Vac. Sci. Technol. B* **11**, 1738(1993). We use a cubic mesh with discretization distance of 0.13575 nm, and 32 × 32 and 64 × 64 planar supercells in this work.

[6] R. Tsu and L Esaki, *Appl. Phys. Lett.* **22**, 562(1973).

[7] J. L. Alay and M. Hirose, *J. Appl. Phys.* **81**, 1606(1997).

[8] R. Sugino, T. Nakanishi, K. Takasaki, and T. Ito, *J. Electrochem. Soc.* **143**, 2691(1996).